Proceedings of the
Annual Stability Conference
Structural Stability Research Council
St. Louis, Missouri, April 16-20, 2013

Performance of Steel Shear Tab Connections at Elevated Temperatures

M.S. Seif[1], J.A. Main[2], T.P. McAllister[3]

Abstract
At the present time, there is a lack of understanding of the performance of structures as complete systems under extreme loading conditions such as realistic, uncontrolled fires. Current specifications for the design of steel structures in the U.S. do not require structural engineers to design for fire conditions. A key issue in evaluating the response of structural systems to fire effects is the response of the structural system, including connections. The typical design procedure of representing connections as fixed or pinned is inadequate when evaluating structural response to fire. This paper presents a first step towards developing a simplified representation of simple shear tab connections for use in structural analysis and design. First, recently developed temperature-dependent material models for different types of steels are implemented. Finite Element (FE) analyses of coupon models are performed to verify the implementation of these material models. Detailed, solid-element models of simple shear tab connections are developed, and analyses are performed to determine the failure modes at different temperatures. The failure modes and key features in the detailed model will be used to develop reduced models of shear tab connections for finite element analyses.

1. Introduction

There is a lack of tools for modeling the response of structural system response, including connections, to realistic, uncontrolled fires. Fire protection of steel structures is usually provided through prescriptive requirements based on the standard fire test (ASTM 2011) which has changed little since it was introduced in 1917. Such tests typically characterize heat transmission through elements and subsystems, but do not provide information about structural performance in real fire. A fuller understanding of the problem will lead to the development of analytical tools and design standards that explicitly consider realistic fire loading for both the design of new buildings and assessment and retrofit of existing ones. Development of design tools usually requires finite element (FE) analyses that consider all failure modes, including local buckling, at elevated temperatures. The work presented here is a first step towards achieving such a

[1] Research Structural Engineer, National Institute of Standards and Technology, Gaithersburg, MD 20899, mina.seif@nist.gov
[2] Research Structural Engineer, National Institute of Standards and Technology, Gaithersburg, MD 20899, joseph.main@nist.gov
[3] Research Structural Engineer, National Institute of Standards and Technology, Gaithersburg, MD 20899, therese.mcallister@nist.gov

capability, where failure modes of single-plate shear connections are simulated with detailed FE analyses. These analyses will be used to formulate reduced connection models that can be used at ambient and elevated temperatures in FE analyses of structural systems.

Single-plate shear connections ("shear tab" connections) are typically designed to resist vertical shear loads for ambient temperatures. However, during exposure to fire, large axial compressive and/or tensile forces may develop in floor beams and their connections. A number of researchers have studied the effect of fire on shear tab connections. Sarraj et al. (2007) developed detailed solid element models for shear tab connections with two to seven bolts to evaluate bolt shearing and bearing behavior. The test specimens that were used for model validation developed tensile forces in the connection as the beam heated. Yu et al. (2009) performed an experimental investigation of the behavior of shear tab connections to vertical shear and tensile forces at elevated temperatures and measured the moment-rotation capacity of the shear tab connections. Simplified models of the shear tab connections were compared against the test data and predicted the failure of 2 of 3 bolts in a connection at elevated temperatures, but under-predicted the connection strength at ambient temperatures. Wald et al. (2009) studied the horizontal forces that developed in steel structures tested in fires. Selamet and Garlock (2010) investigated various ways to retrofit shear connections to improve their performance at elevated temperatures.

This paper presents a study employing FE analysis with geometric and material nonlinearities, using solid and shell elements to model the failure modes of simple shear tab connections in response to elevated temperatures. Recently developed temperature-dependent material models for different types of steels used in shear tab connections are implemented. FE analyses of coupon models are performed to verify the implementation of these material models. Results are presented that illustrate the detailed modeling of the connection and the failure modes under varying load and temperature conditions.

2. Temperature-Dependent Material Modeling

Luecke et al. (2013) have developed an empirical model that provides temperature-dependent material models for any structural steel. The model is based on experiments conducted at the National Institute of Standards and Technology (NIST) and experimental data gathered from literature, including post-yield behavior. The model accounts for the change in yield strength and post-yield strain hardening with temperature.

The elastic modulus E (in GPa) is expressed a function of the temperature T (in °C) as follows:

$$E(T) = E_0 - 4.326\times10^{-2}T - 3.502\times10^{-5}T^2 - 6.592\times10^{-8}T^3 \quad (1)$$

where E_0 = 206 GPa (2987 ksi) is the value at ambient temperature. The temperature-dependence of the yield strength F_y is expressed as:

$$F_y(T) = F_{y0}\cdot\exp\left(-\frac{1}{2}\left(\frac{\Delta T}{b}\right)^a - \frac{1}{2}\left(\frac{\Delta T}{d}\right)^c\right) \quad (2)$$

where F_{y0} is the yield strength at ambient temperature, ΔT (in °C) is the increase in temperature above the ambient temperature, and a, b, c, and d are coefficients depending on the type of steel. For rolled structural steel, $a = 5.708$, $b = 1.000$ °C, $c = 590$, and $d = 919$ °C, while for bolts, $a = 4.967$, $b = 1.000$ °C, $c = 456$, and $d = 2040$ °C. Fig. 1 shows the degradation of the normalized yield strength with increasing temperature for ASTM A572 rolled steel and ASTM A325 and A490 bolts, using Eq. (2) with the coefficients listed previously.

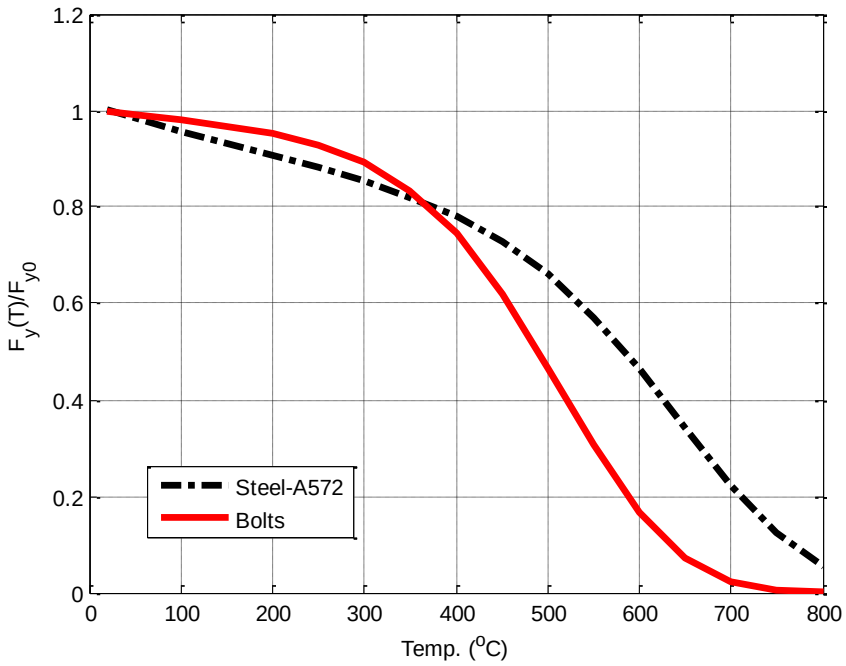

Figure 1. Degradation of normalized yield strength versus the increase in temperature for rolled structural steel and bolts.

The true stress σ_{true} is expressed as a function of true strain ε_{true} as follows:

$$\sigma_{true} = \begin{cases} E\varepsilon_{true} & \text{for } \varepsilon_{true} < F_y / E \\ \left(F_y + (959 - 0.766F_{y0}) \exp\left(-\left(\frac{T}{538} \right)^{8.294} \right) \left(\varepsilon_{true} - F_y / E \right)^{0.483} \right) & \text{for } \varepsilon_{true} \geq F_y / E \end{cases} \quad (3)$$

where it is noted that E and F_y depend on temperature according to Eqs. (1) and (2). Fig. 2 shows the true stress-strain curves for the A572 steel, generated using this temperature-dependent material model.

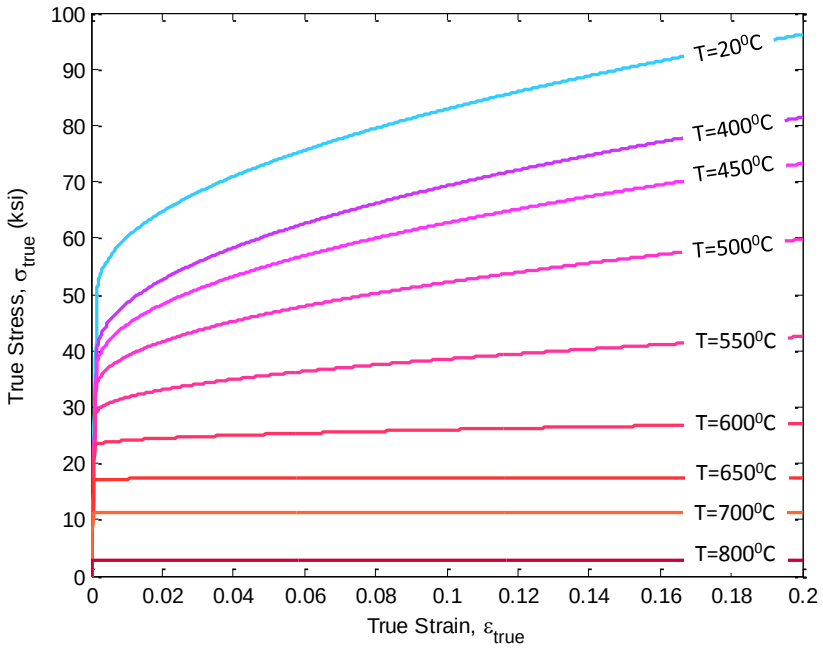

Figure 2. True stress-strain curves for A572 steel, generated with Luecke et al. (2013) temperature-dependent material model (1 ksi = 6.895 MPa).

3. Finite Element Analysis of Uniaxial Tension

The temperature-dependent material model described in Section 2 is used subsequently for finite element (FE) analysis of shear tab connections at elevated temperatures. In order to verify that the FE software accurately captures the behavior of the temperature-dependent material model under uniaxial tension, since the simulated behavior is dependent on finite element type and size, FE analyses of tensile coupons were performed and are compared to the empirical material model presented in Section 2. Comparisons were performed on coupons modeled with solid and shell elements, as shown in Fig. 3, with element formulations and mesh sizes consistent with the solid and shell elements used in the analyses of shear tab connections presented subsequently.

The analyses were performed using the LS-DYNA FE software (LSTC 2012) with explicit time integration. The empirical material model was implemented using material type 106 in LS-DYNA, an elastic viscoplastic material model with thermal effects. A family of true stress versus plastic strain curves at different temperatures was provided as input to the model, and these curves were generated using Eq. (3) with values of plastic strain obtained by subtracting the elastic strain from the true strain. Fracture was modeled using element erosion, in which elements were removed from the analysis when a specified value of effective plastic strain was reached. In the analyses presented in this paper, a temperature-independent plastic strain value of 0.5 was used as the erosion criterion for all steel materials.

Fig. 4 shows engineering stress-strain curves calculated from the empirical material model (listed as input) and the computed engineering-stress strain curves from the shell and solid element coupon simulations, at 20 °C, 200 °C, 400 °C, and 600 °C. Engineering stress values were obtained from the analysis results by dividing the total axial force by the initial cross-sectional area of the coupon, and engineering strain values were obtained by dividing values of extension by the initial gauge length of 2 in (50.8 mm). True stress-strain curves from the empirical model

were transformed to engineering stress-strain curves for comparison with the analysis results. The results show that the stress-strain curves obtained from the solid element coupon models are almost identical to the empirical material model for all four temperatures (less than 1 % difference at 20 % strain). For the shell element coupon models, the stresses at higher strains are slightly higher than those of the empirical material model (up to 8 % higher at 20 % strain), because stresses in the shell element formulation do not account for changes in thickness caused by the Poisson effect. These discrepancies at high strains for the shell elements do not affect the analysis results presented subsequently for shear tab connections, because shell elements are used to model the beam section away from the connection where the strains remain small. Regions with large strains are modeled with solid elements.

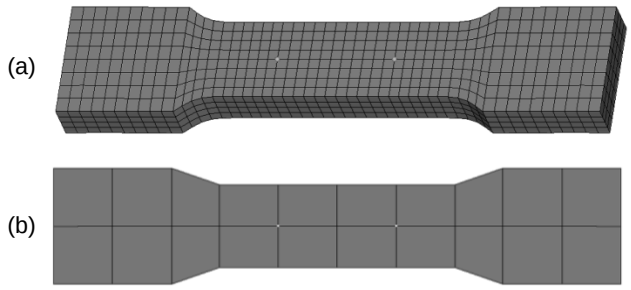

Figure 3. Sample finite element models of tensile coupons: (a) solid elements; (b) shell elements

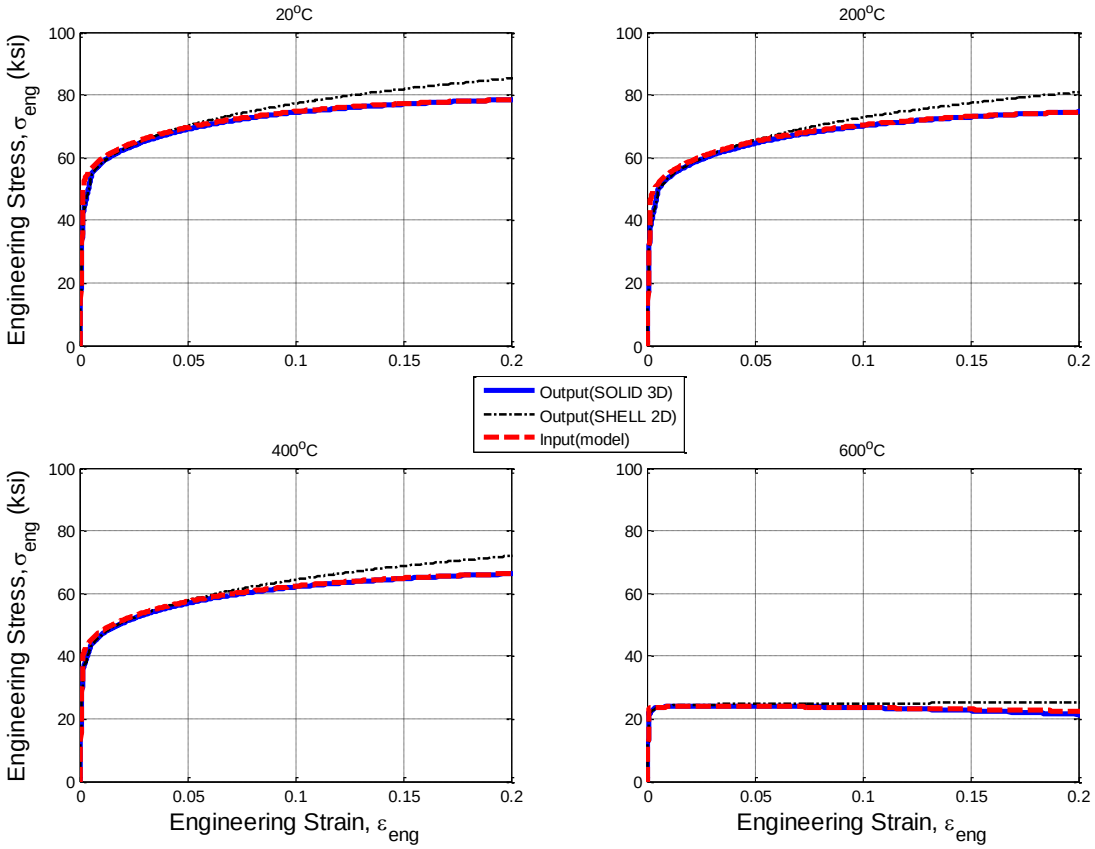

Figure 4. Engineering stress-strain curves for the temperature-dependent material model (input), and the solid and shell element tensile coupon simulations (1 ksi = 6.895 MPa).

4. Shear Tab Connections

4.1. Prototype Building

Fig. 5a shows the plan view of a prototype, 10-story, steel-frame building described in Main and Sadek (2012), designed for gravity loads corresponding to office occupancy and seismic loads for Seismic Design Category C. Lateral loads are resisted by seismically designed intermediate moment frames on the exterior of the building. All interior frames are designed to support gravity loads only, assuming fully composite action between the steel beams and the concrete slab. Grade 50 structural steel is used in the beams and columns, and beams in the gravity frames are connected to the columns using shear tab connections, illustrated in Fig. 5b. The shear connection details shown in Fig. 5b are used for both the W16x26 girders in the north-south direction and the W14x22 beams in the east-west direction of the gravity framing system. In this study, a connection from an east-west beam, with a span length of 30 ft (9.14 m), is selected for analysis.

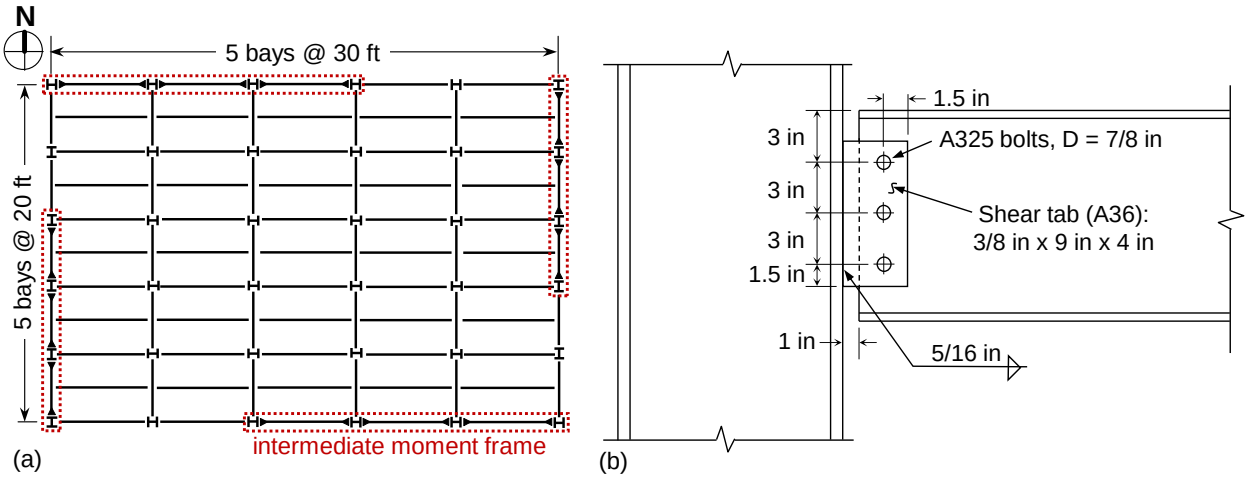

Figure 5. (a) Plan view of prototype building; (b) details of single-plate shear connections (1 ft = 0.3048 m, 1 in = 25.4 mm).

4.2. Analysis Approach

Detailed nonlinear FE analyses were conducted to simulate the failure modes of the shear tab connections under elevated temperatures. In each analysis, the connection was subjected to the prescribed axial displacement cycle shown in Fig. 6, in which positive (compressive) displacements are followed by negative (tensile) displacements. Analyses were performed using explicit time integration in LS-DYNA (LSTC 2012), and the smooth functional form of the prescribed displacement curve in Fig. 6b was developed to ensure that dynamic effects are negligible (i.e., to ensure quasi-static loading conditions) while subjecting the connection to the desired range of motion. The alternating compressive and tensile stages of loading are of interest because they represent the types of loading imposed on connections in the heating and cooling phases of a fire, respectively. The maximum compressive displacement of 1 in (25.4 mm) corresponds to displacement at which the beam begins to bear against the column (see Fig. 5b). While the displacements imposed on a connection in a realistic fire depend on the temperature distribution within the structural elements and the thermal restraint imposed by the structural

configuration, the simple loading protocol considered here enables investigation of the behavior, failure modes, and ultimate capacities of the connections at different temperatures. In later phases of this project, reduced connection models that capture these temperature-dependent failure modes can be used in analysis of composite floor systems under realistic fire loading.

Analyses under the prescribed displacement protocol in Fig. 6 were performed at four different temperatures (20 °C, 200 °C, 400 °C, and 600 °C), with the temperature in each analysis being uniform and constant. The first set of analyses considered axial loading only, and a second set was performed in which a vertical shear load was applied to the free end of the beam, representing the service-level gravity loads carried by the connection, followed by the prescribed axial displacement.

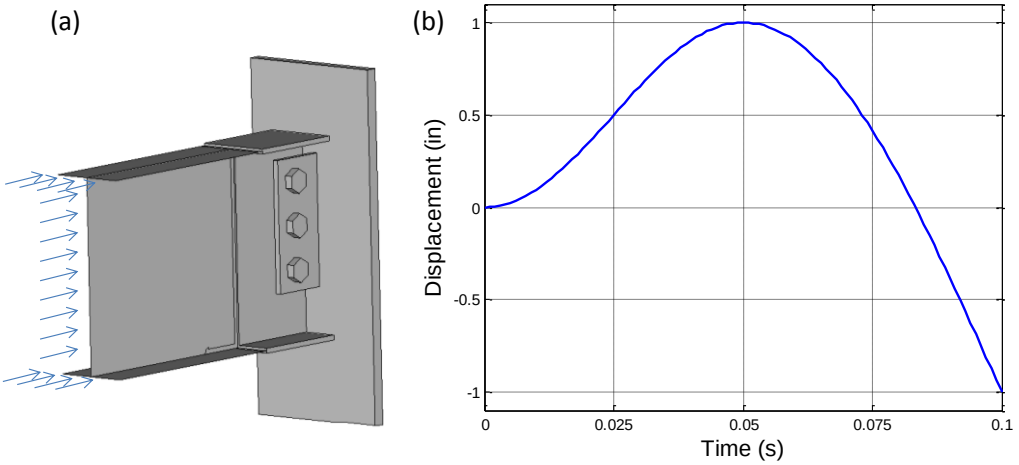

Figure 6. Displacement applied on the connection (a) 3D sketch, (b) prescribed displacement curve (1 in = 25.4 mm).

4.3. Mesh and Element Selection

The shear tab was modeled using finely meshed three-dimensional solid elements for modeling the beam, bolts, shear tab, and column. Fully integrated eight node elements were used for the solid elements. A typical element size of 0.12 in (3 mm) was used for the meshing of the beam (three layers of elements across the web and across the flanges) and the shear tab (four elements across the thickness). A finer mesh with a typical element size of 0.06 in (1.5 mm) was used to mesh the bolts. The bolt holes in the beam web and shear tab were modeled as standard hole sizes, with a diameter $^{1}\!/_{16}$ in (1.6 mm) larger than the bolt diameter. Contact was defined between the bolts, shear tab, and beam web to model the transfer of forces through the bolted connection, including friction, with a value of 0.3 assumed for both the static and dynamic coefficients of friction. The free end of the beam was modeled using two dimensional shell elements, with constraints tying the edges of the shell elements to the nodes of the solid elements at their interface. Fully integrated four node shell elements were used, with five integration points through the shell thickness. A typical model showing the mesh density is presented in Figure 7 (the column and free end of the beam are omitted from the figure for clarity).

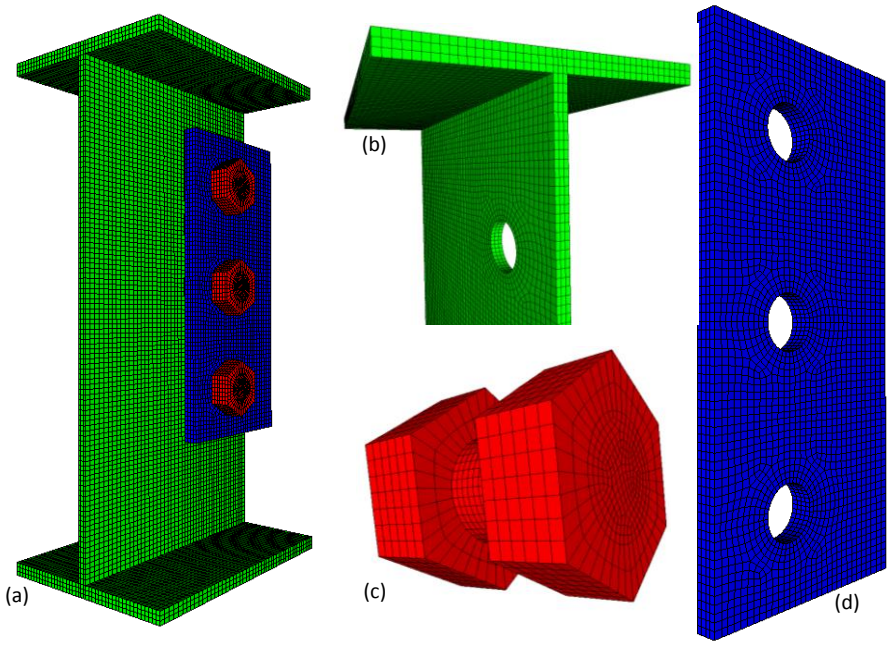

Figure 7. Shear tab connection detailed model (a) full model, (b) beam, (c) bolt, and (d) shear tab.

4.4. Material Modeling

The steel materials were modeled as described previously in Section 3, using the temperature-dependent material model equations presented in Section 2. Material model parameters for ASTM A572 Grade 50 steel, with F_{y0} = 50 ksi (345 MPa), were used for modeling the beam and column, while parameters for ASTM A36 steel, with F_{y0} = 36 ksi (250 MPa), were used for the shear tab, and parameters for ASTM A325 bolts, with F_{y0} = 120 ksi (827 MPa), were used for the bolts (see Fig. 5b for connection details). An additional set of analyses were performed using material model parameters for ASTM A490 bolts, with F_{y0} = 130 ksi (896 MPa), to evaluate the effect of increased bolt strength on connection performance at elevated temperatures.

4.5. Results and Discussion

Fig. 8 summarizes the analysis results for the shear tab connection with A325 bolts subjected to axial loading through the prescribed displacement curve shown in Fig. 6b, without vertical shear load. The axial load in the connection is plotted against the prescribed displacement at each temperature (20 °C, 200 °C, 400 °C, and 600 °C). At 20 °C, 200 °C, and 400 °C, the connections reach their peak compressive resistance at a displacement of about 0.13 in (3.3 mm), after which their resistance decreases with increasing displacement, as the beam web buckles locally around the bolt group. This buckling failure mode is illustrated in Fig. 9. While Fig. 9 corresponds to 400 °C, similar failure modes were observed at 20 °C and 200 °C, in which the connection experienced web buckling in the compression part of the loading cycle (i.e., simulating the heating phase of the fire). When the prescribed displacement reaches 1 in (25.4 mm), the gap between the beam and the column closes, and increasing resistance is observed as the beam bears against the column. During the tension part of the loading cycle (i.e., the cooling phase of the fire) tear-out failure occurred in the beam web for temperatures of 20 °C, 200 °C, and 400 °C, as shown in Fig. 10. Tear out in the beam web is expected since the beam web is thinner than the shear tab plate.

As seen in Fig. 8, increasing the connection temperature from 20 °C to 400 °C produced a reduction of 10 % in the connection compressive capacity, while increasing the temperature to 600 °C reduced the capacity by 75 %. At 600 °C, the connections failed due to shear fracture in the bolts (see Fig. 11) during the compression phase of the loading cycle, as the bolt capacity is much less than the capacity of the structural steel at 600 °C (see Fig. 1). The connection loses all of its capacity at a compressive displacement of about 0.2 in (5.08 mm.).

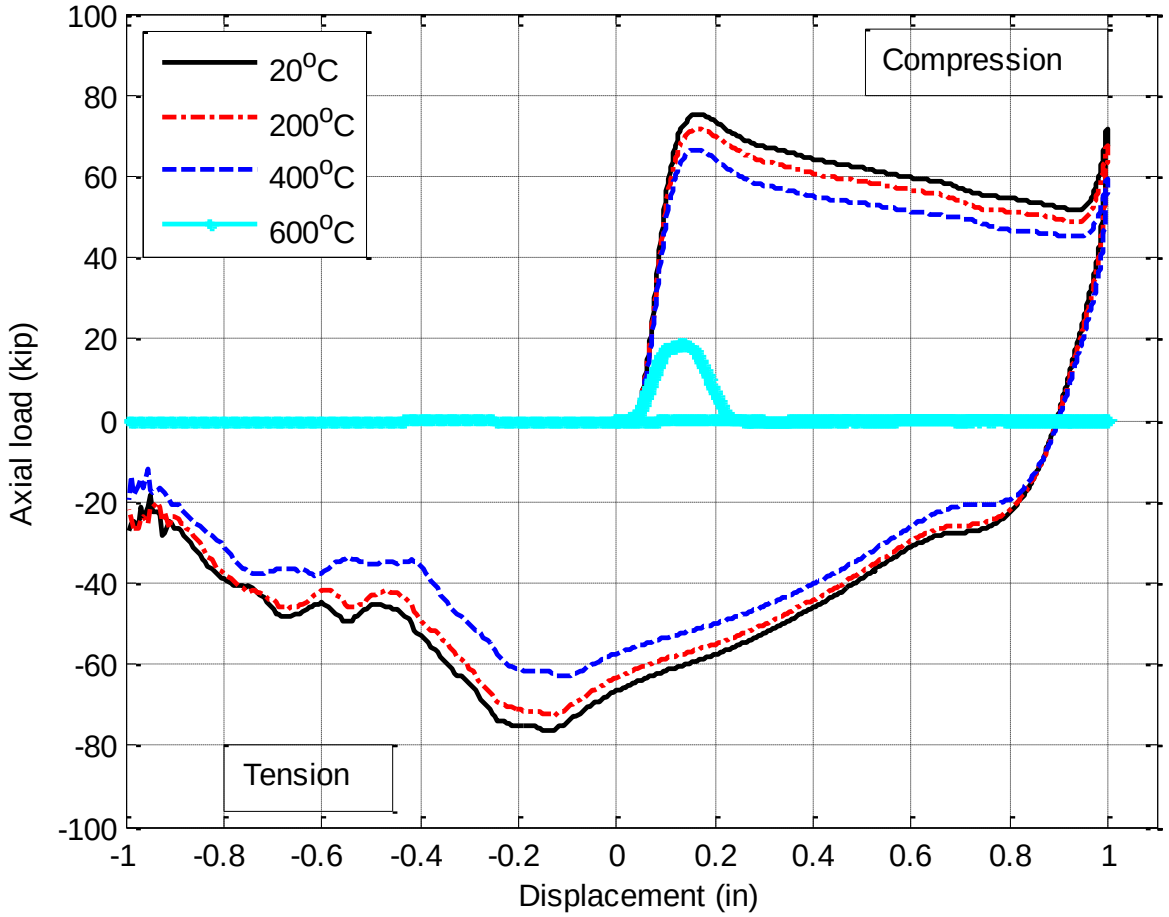

Figure 8. Axial load in the connection versus the prescribed displacement at different temperatures, for the prototype connections with A325 bolts, under displacement loading (1 kip = 4.448 kN, 1 in = 25.4 mm).

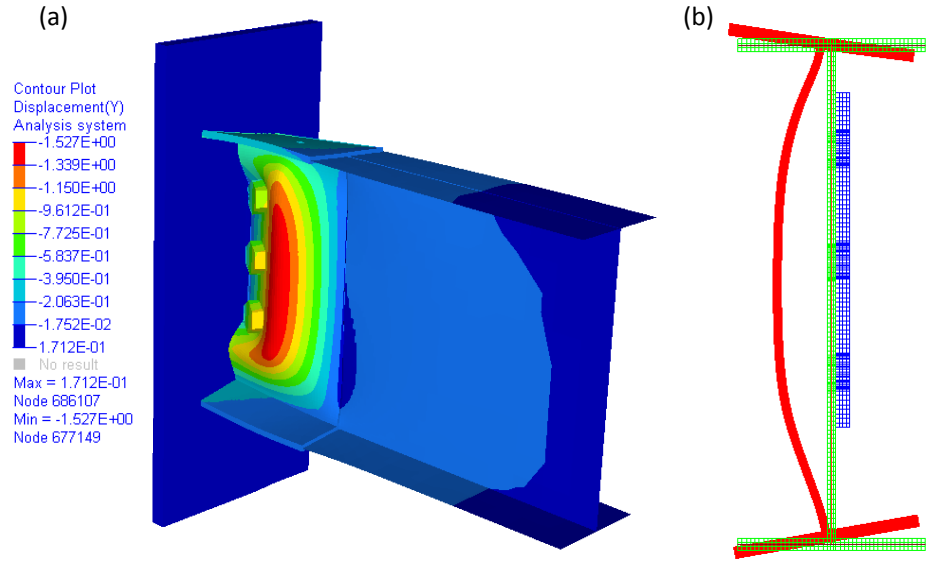

Figure 9. Web buckling failure mode at 400 °C: (a) Perspective view with out-of-plane displacement contours (values in inches, where 1 in = 25.4 mm) and (b) cross-sectional view of undeformed and buckled section.

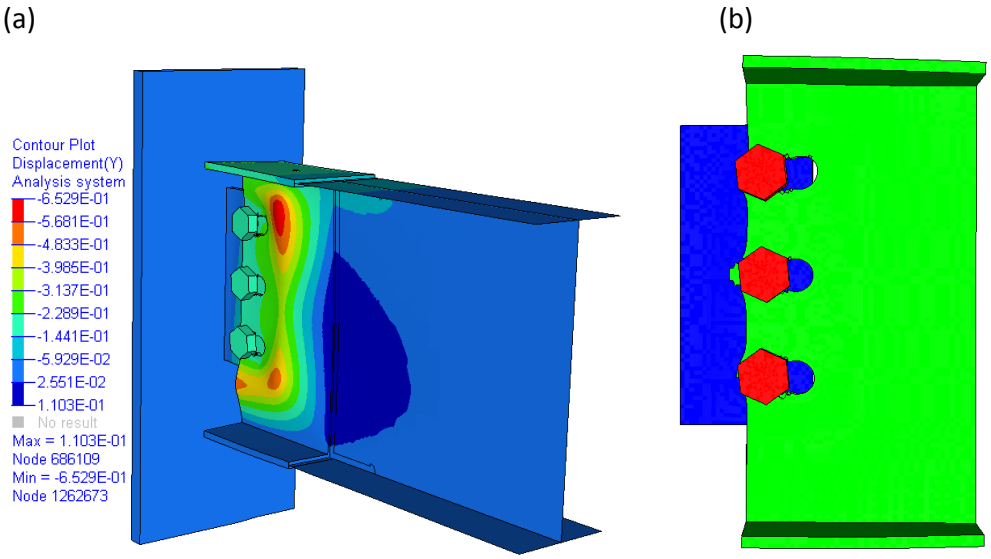

Figure 10. Web tear-out failure mode at 400 °C: (a) Perspective view with out-of-plane displacement contours (values in inches, where 1 in = 25.4 mm) and (b) side view showing tear-out failure of beam's web.

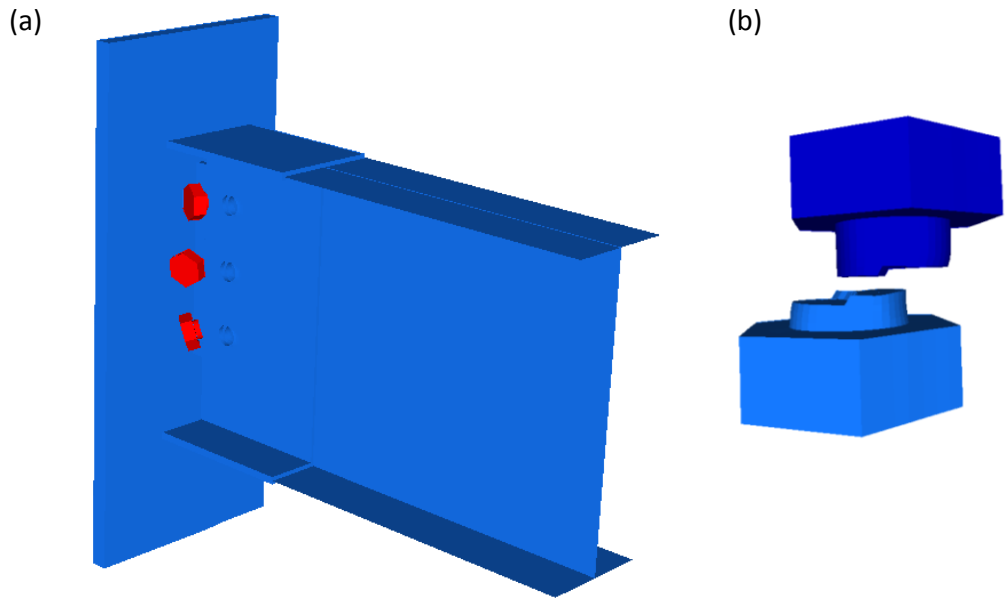

Figure 11. Bolt shear failure mode at 600 °C: (a) Perspective view showing the bolt heads (in red) separating from the connection after shear failure, and (b) top view of a sheared bolt.

Use of A490 bolts did not significantly change the performance of the connection at 20 °C, 200 °C, or 400 °C, as web buckling failure occurred within 9 % of the failure load obtained using A325 bolts. However, bolt shear failure occurred at 600 °C, and the use of A490 bolts increased the connection's capacity by about 37 % and its ductility by about 20 % relative to the capacity with A325 bolts, as shown in Fig. 12.

Adding vertical shear load to the connection, prior to applying the prescribed axial displacement, allowed the connection to carry the load earlier in the loading cycle, since the gaps between the bolts and the bolt holes were closed during application of the vertical shear load, prior to the axial displacement. The vertical shear load did not significantly change the capacity of the connection at 20 °C, 200 °C, or 400 °C (the capacity changed by 10 %). However, at 600 °C, the presence of the vertical shear load reduced the connection capacity by about 50 % and its ductility by about 65 % relative to the connection capacity under axial loading without vertical shear load, as shown in Fig. 12.

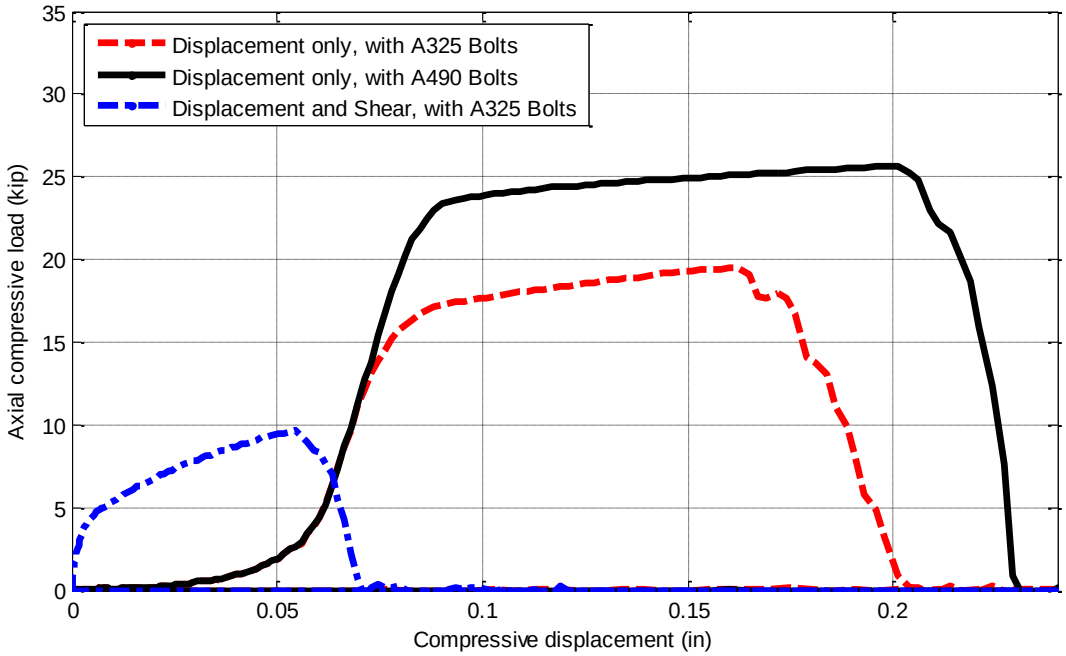

Figure 12. Axial load carried through the connection versus the applied displacement at 600°C for different loading cases and bolt types (1 kip = 4.448 kN, 1 in = 25.4 mm).

5. Concluding Remarks

This paper examined the effect of elevated temperature on the failure modes of simple shear tab connections. A temperature-dependent material model for steel was implemented and evaluated for FE analysis. Nonlinear FE analyses were conducted on a detailed connection models to identify failure modes at elevated temperatures for cases of axial load (displacement controlled, representing the heating and cooling phases under fire loading), and combined shear and axial load.

The results showed the following behavior of shear tab connections at elevated temperatures:

- At 20 °C, 200 °C, and 400 °C, under axial loading, the beam web buckled locally in the compression part of the displacement cycle (representative of the heating phase of the fire), followed by tear-out in the beam web during the tension part of the displacement cycle (representative of the cooling phase of the fire).
- At 600 °C, the connection failed due to shear fracture in the bolts during the compression phase of the displacement cycle.
- Increasing the steel temperature from 20 °C to 400 °C, produced a reduction of 10 % in the connection capacity; increasing the temperature to 600 °C from 20 °C reduced the capacity by 75 %.
- The use of A490 bolts rather than A325 bolts did not significantly change the performance of the connection at 20 °C, 200 °C, or 400 °C. However, at 600 °C when bolt shear failure occurs, A490 bolts increased the connection capacity by about 37 % and its ductility by about 20 % relative to the connection capacity with A325 bolts.

- Adding a vertical shear load to the connection, prior to applying the prescribed axial displacement, resulted in earlier loading since the gap between the bolts and the bolt holes were closed during application of the shear loading. The inclusion of the vertical shear load did not significantly change the capacity of the connection at 20 °C, 200 °C, or 400 °C. However, at 600 °C, the vertical shear load reduced the connection capacity by about 50 % and its ductility by about 35 % relative to the capacity under axial displacement without vertical shear load.

The work herein represents a first step towards simulating all failure modes for shear tab connections under fire loading, including local buckling. These FE analyses study the effect of axial and shear loading conditions and elevated temperatures on connection failure modes. The ultimate goal of this research is to provide reduced connection models for the analysis and design of structural systems under ambient conditions and fire loading.

Disclaimer

Certain commercial software or materials are identified to describe a procedure or concept adequately; such identification is not intended to imply recommendation, endorsement, or implication by the National Institute of Standards and Technology (NIST) that the software or materials are necessarily the best available for the purpose.

References

AISC (2010). "Specification for Structural Steel Buildings", *American Institute of Steel Construction*, One East Wacker Drive Suite 700, Chicago, IL 60601-1802. ANSI/ASIC 360-10.

ASTM (2011), "ASTM Standard E119-11a Standard Test Methods for Fire Tests of Building Construction and Materials", *ASTM International*, West Conshohocken, PA, 2009, DOI: 10.1520/E0119-11A.

Garlock M.E., Selamet S. (2010). "Modeling and behavior of steel plate connections subject to various fire scenarios", *Journal of Structural Engineering*, Vol 137(7), 2010, pp 897-906.

Livermore Software Technology Corporation (LSTC). (2012), "LS-DYNA Keyword User's Manual." Livermore, CA.

Luecke W., Gross J.L., McColskey J.D. (2013). "High-temperature, tensile, constitutive models for structural steel in fire", AISC *Engineering Journal*, (Submitted).

Main J.A., Sadek F. (2012). "*Robustness of Steel Gravity Frame Systems with Single-Plate Shear Connections"*. NIST TN 1749, National Institute of Standards and Technology. Gaithersburg, MD, May, 2012.

Sarraj M., Burgess I.W., Davison J.B., Plank R.J. (2007). "Finite element modeling of steel fin plate connections in fire", *fire Safety Journal*, Vol 42, 2007, pp 408-415.

Selamet S., Garlock M.E. (2010). "Robust fire design of single plate shear connections", *Engineering Structures*, Vol 32, 2010, pp 2367-2378.

Wald F., Sokol Z., Moore D. (2009). "Horizontal forces in steel structures tested in fire", *Journal of Constructional Steel Research*, Vol 65, 2009, pp 1896-1903.

Yu H., Burgess I.W., Davison J.B., Plank R.J. (2009). "Experimental investigation of the behavior of fin plate connections in fire", *Journal of Constructional Steel Research*, Vol 65, 2009, pp 723-736.